NOTES AND CORRESPONDENCE

The Mechanism for Antarctic Intermediate Water Renewal in a World Ocean Model

MATTHEW H. ENGLAND

Department of Geology and Geophysics, The University of Sydney, Sydney, Australia

J. STUART GODFREY

CSIRO Division of Oceanography, Hobart, Tasmania, Australia

ANTHONY C. HIRST

CSIRO Division of Atmospheric Research, Aspendale, Victoria, Australia

MATTHIAS TOMCZAK

School of Earth Sciences, Flinders University, Adelaide, S.A., Australia

15 May 1992 and 23 September 1992

ABSTRACT

Realistic representation of the low-salinity tongue of Antarctic Intermediate Water (AAIW) has been achieved in a coarse-resolution ocean general circulation model. The authors find that this water mass is not generated by direct subduction of surface water near the polar front. Instead, the renewal process is concentrated in the southeast Pacific Ocean off southern Chile. The outflow of the East Australian Current progressively cools (by heat loss to the atmosphere) and freshens (by assimilation of polar water, carried north by the surface Ekman drift) during its slow movement across the South Pacific toward the AAIW formation zone. Further, deep, warm advection near Chile enables more convective overturn, resulting in very deep mixed layers from which AAIW is fed into the South Pacific and also into the Malvinas Current. Along with this isolated region of AAIW renewal, the model relies on alongisopycnal mixing of fresh surface water from the polar front to capture a realistic circumpolar tongue of low salinity water at 1000-m depth.

1. Introduction

The study of the formation of the World Ocean water masses is intimately linked to the study of the earth's climate through the global-scale transports of heat and fresh water in the oceans. Furthermore, the time scale for anthropogenic changes in the world's environment is controlled by the ocean because of its enormous capacity to store heat. The World Ocean circulation at its largest scale is often thought of in terms of the gradual renewal or ventilation of the deep ocean by water that was once at the sea surface (e.g., Gordon 1986; Broecker 1991). Our knowledge of the exact renewal processes operating in the deep and intermediate waters of the World Ocean is still somewhat limited, particularly in the Southern Ocean. This is because the measurement of processes that determine the ocean's ventilation (e.g., deep convective overturn, vertical motion, abyssal currents, and mesoscale diffusion) is not feasible on a basin-to-global scale. General circulation models of the ocean provide a unique opportunity to understand the ventilation and renewal processes operating in the World Ocean. This study focuses on the renewal mechanism operating in the intermediate waters of the Southern Ocean in a global-scale ocean general circulation model.

A major feature of Southern Ocean hydrography is a pronounced salinity minimum at intermediate depths (Deacon 1937; and Fig. 1a). The associated water mass, known as Antarctic Intermediate Water (AAIW), is characterized by a relatively low salinity tongue (about 34.4 psu at 1000-m depth) that *appears* to originate near the surface at about 60°S, spreading equatorward at about 1000-m depth. It was first suggested (Sverdrup et al. 1942) that AAIW formation occurs *circumpolarily* by cross-polar frontal mixing of low salinity Antarctic Surface Water and Subantarctic Upper Water. The form of the tongue in Fig. 1a might suggest that alongisopycnal subduction is taking place, since

Corresponding author address: Dr. Matthew H. England, GRGS/CNRS, 18 Avenue Edouard Belin, Toulouse, Cedex, France 31055.

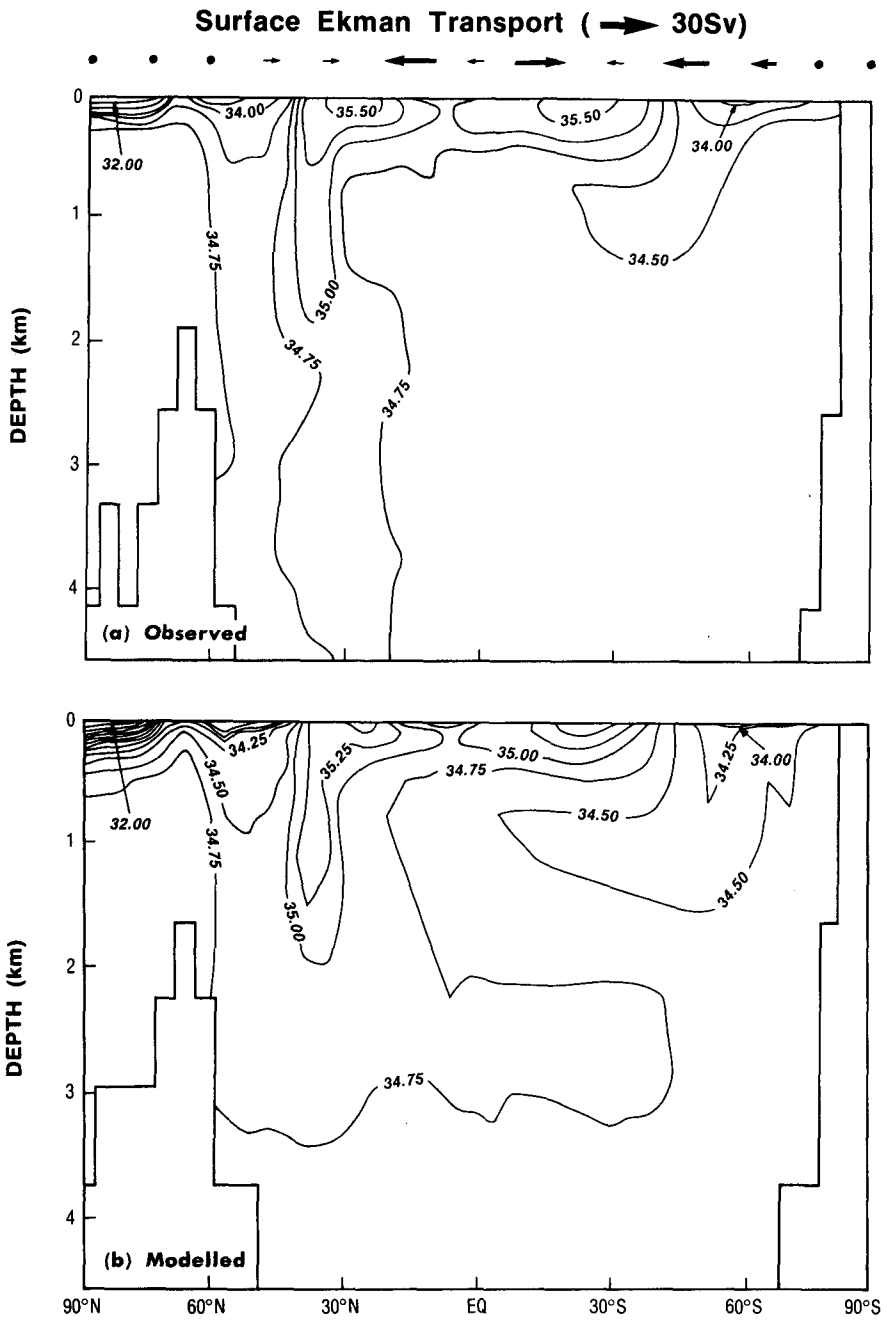

FIG. 1. (a) Observed and (b) simulated zonally averaged latitude–depth section of salinity in the World Ocean. Contour interval is 0.25 psu. Vectors at the top of the diagram indicate the zonally integrated strength of surface Ekman transport in Sverdrups (1 Sv $\equiv 1 \times 10^6$ m^3 s^{-1}).

salinity represents a good tracer of ocean circulation at midlatitudes. However, this seems somewhat unlikely, in view of the strong divergence of the zonally integrated Ekman transport at this latitude (Fig. 1); this clearly suggests near-surface upwelling near 60°S. Mixing would have to be remarkably vigorous to create the salinity tongue of Fig. 1 in the face of this upwelling. McCartney (1977, 1982) suggested instead that AAIW principally originates in a localized region near Cape Horn, as the deepest, densest, and most prolific of a sequence of water masses he called "Subantarctic Mode Waters."

The representation of AAIW is generally poor in prognostic models of the World Ocean (e.g., Toggweiler et al. 1989) and in coupled models of the ocean–atmosphere system (England et al. 1992). England

(1992, 1993) has shown recently that an AAIW tongue can quite successfully be simulated when a coarse-resolution ocean GCM is run to steady state, provided appropriate attention is given to observed wintertime salinities near Antarctica and to the detailed shape of the Drake Passage, and provided that an isopycnal mixing scheme is incorporated into the model; Fig. 1b is from this simulation. Here we describe the mechanism of AAIW formation in England's model. It strongly supports McCartney's suggestions, but it also suggests that alongisopycnal mixing is in fact strong enough to be an important contributor to the overall process of AAIW formation, despite the upwelling that does occur south of the Antarctic Circumpolar Front in the model.

While the focus of this note is on the AAIW renewal process obtained in the World Ocean model reported by England (1993), it is worth mentioning that an independent modeling effort by Hirst and Godfrey (1993) obtained largely similar dynamical processes in the Southern Ocean as those described here. While their study employs the same basic primitive equation model used by England (1993), they have higher horizontal resolution, a different set of bulk mixing parameters, and a more realistic ocean bathymetry (e.g., the circulation around New Zealand is resolved).

2. The World Ocean model

The ocean model employed by England (1993) is the so-called Bryan–Cox primitive equation numerical model (Bryan 1969; Cox 1984; Pacanowski et al. 1991). The configuration of the model has a global coverage of the ocean, with a realistic approximation of bottom bathymetry and continental boundaries. The grid spacing is 3.75° longitude by 4.5° latitude with 12 vertical levels. Because of the coarse horizontal and vertical resolution, the effects of mesoscale eddies are only taken into account implicitly by approximate closure schemes. While the mixing of tracers necessarily takes place in Cartesian coordinates (for numerical stability), an isopycnal mixing scheme (Redi 1982) is also incorporated that more realistically represents the tendency for heat and salt to be mixed on surfaces of constant density. The ocean is forced at the sea surface by annual-mean climatological boundary conditions of temperature–salinity (Levitus 1982) and wind stress (Hellerman and Rosenstein 1983). The surface thermohaline conditions are prescribed via a Newtonian restoring term (Haney 1971), with a temperature relaxation constant of $(30 \text{ days})^{-1}$ (or equivalently $\lambda \approx 75 \text{ W m}^{-2} \text{ °C}^{-1}$, after Haney 1971). In the extreme Southern Ocean (south of 70°S), the surface salinity forcing is adjusted to crudely represent the process of wintertime sea ice formation off Antarctica. During June to August of each year, the southernmost row of ocean grid points is restored toward a maximum value of 35.0 psu, with a smooth interpolation defining the enhanced forcing at the remaining latitudes up to 70°S. The maximum surface salinity chosen matches estimates of the wintertime salinity of shelf water in the Ross and Weddell seas (Jacobs et al. 1985; Foster and Carmack 1976), when sea ice formation rejects salt into the water column.

The ocean model was integrated out for the equivalent of several thousand years at the surface, by which time a steady-state solution had been reached. The analysis presented here is based on the annually averaged ocean state reached at the end of the model integration. The only time-dependent aspect of the converged solution is related to the periodic enhancement of surface salinities in the extreme Southern Ocean. This results in wintertime episodes of deep convective overturn of the model equivalent of Antarctic Bottom Water.

3. The renewal mechanism for AAIW

The observed and simulated salinity at 1000 m and 1131 m, respectively, (Fig. 2) each show two minima: one west of Cape Horn and the second off Argentina. These minima are likely to lie close to the principal source regions of AAIW. The model velocity field at 1131 m (Fig. 2c) supports this idea: flows can be seen moving northwest, then west from southern Chile, to supply water from the first salinity minimum to much of the south Pacific, while the second salinity minimum of Fig. 2b coincides with the outflow of the Malvinas Current. The heavy dashed lines in Fig. 3 indicate where water with $\sigma_t = 27.1 \text{ kg m}^{-3}$, coinciding in the model with the core of AAIW, breaks the surface in the Southern Hemisphere. It can be seen in the model that this line generally lies in a region with no surface downwelling (Fig. 3a) or convective overturn (Fig. 3c), and positive heat flux into the ocean (Fig. 3b); it is thus not a region of deep water mass formation by direct subduction or convective adjustment.

It remains to be shown why, in the model, AAIW is formed in such a concentrated region off South America, and also why a continuous tongue of low salinity is simulated at all longitudes in spite of the ambient upwelling near 60°S. Figure 3b shows the net surface heat flux in the model. Heat loss from the Pacific is seen to occur in three main bands that come together off southern Chile. The northernmost band occurs in regions where the surface flow (Fig. 4a) has a southward component, bringing it into regions of cooler equilibrium temperature; this southward flow is due to Ekman transports induced by the trade winds and is not found one level farther down (Fig. 4b). This band of surface heat loss does not result in any formation of convective mixed layers (Fig. 3c). The southernmost band of heat loss in Fig. 3b involves convective overturn near Antarctica, creating water masses much colder and denser than AAIW that ultimately ventilate the bottom of the model ocean.

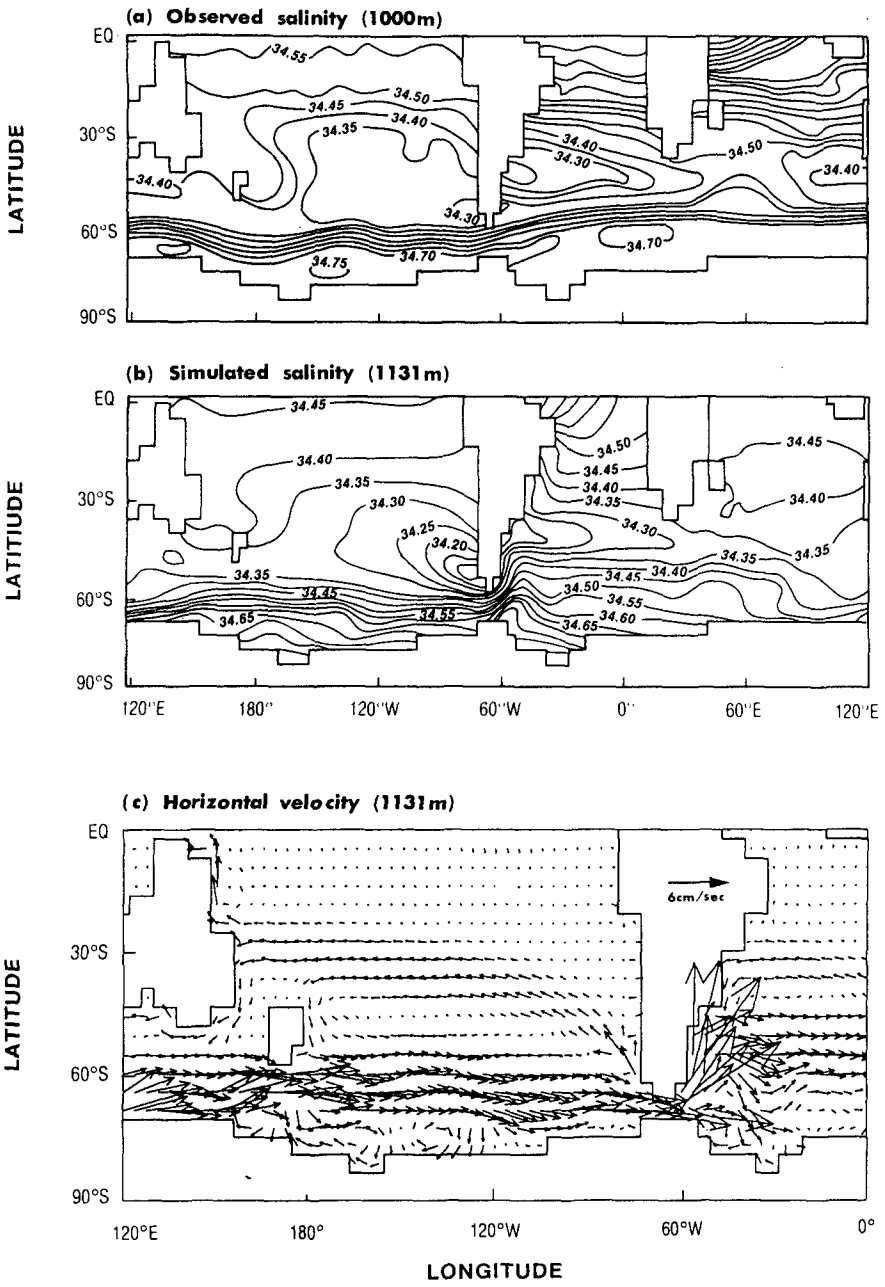

FIG. 2. (a) Observed long-term annual mean salinity at 1000-m depth redrafted from Levitus (1982). (b) Salinity at 1131-m depth (level 7) in the ocean model. (c) Horizontal velocity at 1131-m depth in the ocean model.

By contrast, the middle band of heat loss in Fig. 3b coincides in the model with a band of convective overturn whose depth increases steadily eastward from southeast Australia to southern Chile (Fig. 3c). Heat flux climatologies (Esbenson and Kushnir 1981; Oberhuber 1988) show no data in this region, so we have no direct evidence to confirm the existence of this band of ocean heat loss. However, McCartney (1977) and Molinelli (1978) both note the existence of deep mixed layers just north of the Antarctic Circumpolar Front in direct ocean measurements, which is where they are located in Fig. 3c. McCartney (1977) associated this band with the formation of Subantarctic mode water. Such deep mixed layers probably imply that a band of heat loss to the atmosphere does exist in this region. Just below the surface Ekman layer, water is seen to enter this band from the WNW along Australia's south coast (Fig. 4b), and (more prominently) from the north

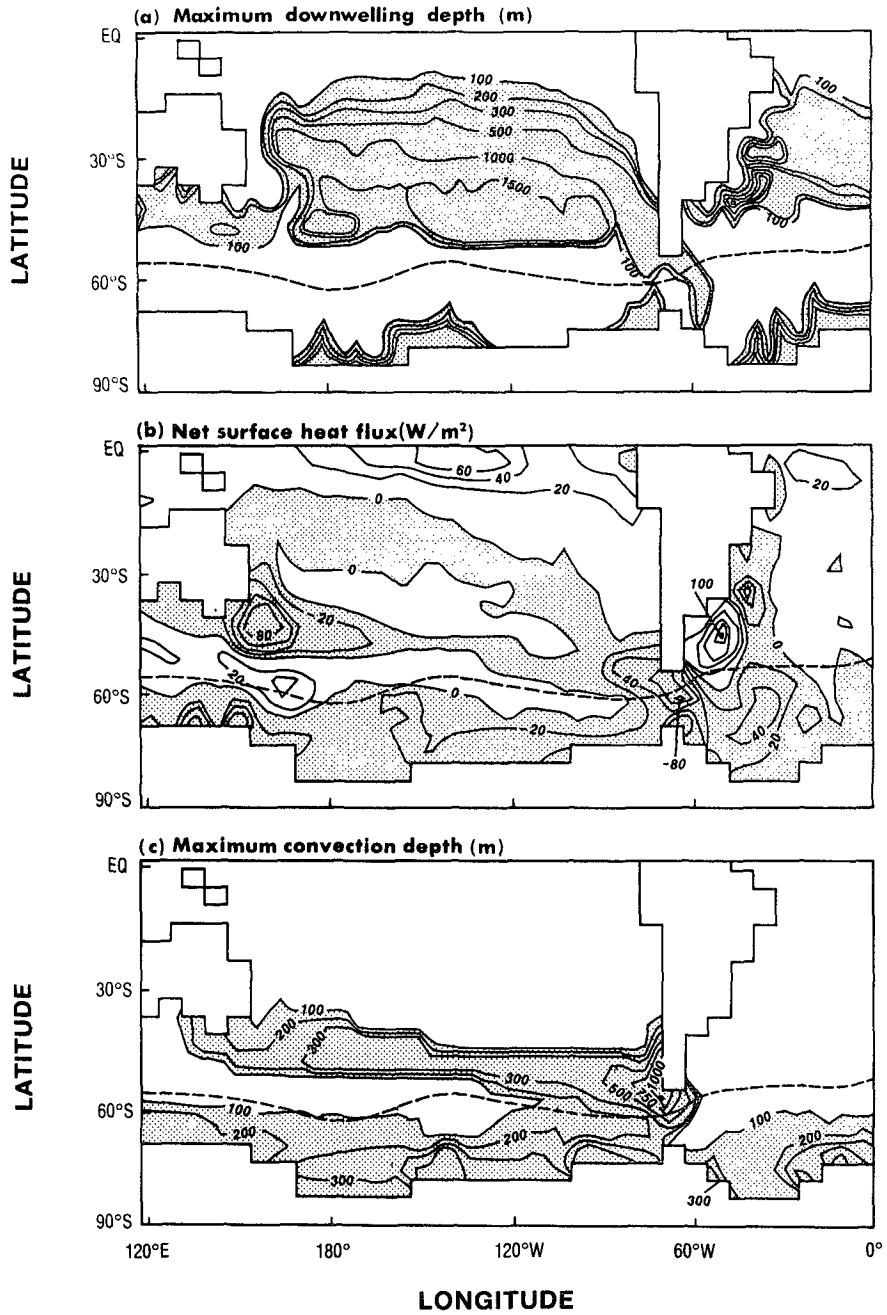

FIG. 3. (a) The maximum depth (m) reached by direct downwelling of surface water in the South Pacific and southwest Atlantic oceans. (b) Annually averaged net surface heat flux (W m^{-2}) into the model ocean. (c) As in (b) but showing the maximum depth (m) of water overturned by convective adjustment of properties from the surface. The dashed line near 60°S indicates where the σ_t = 27.1 kg m^{-3} density surface breaks the sea surface.

in the East Australian Current. This latter inflow, which is warmer than the surface equilibrium temperature of 11°C at 45°S, then flows ESE, directly along the middle band of heat loss in Fig. 3b (note that New Zealand has been turned into a seamount in the interests of computational convenience). A similar flow pattern can be seen east of New Zealand in Fig. 2c: water flows south with the New Zealand western boundary current, then proceeds directly ESE along the axis of the middle band of heat loss of Fig. 3b. Similar flows are found at intermediate depths; thus the entire top 1000 m of the water column appears to advect along the axis of heat

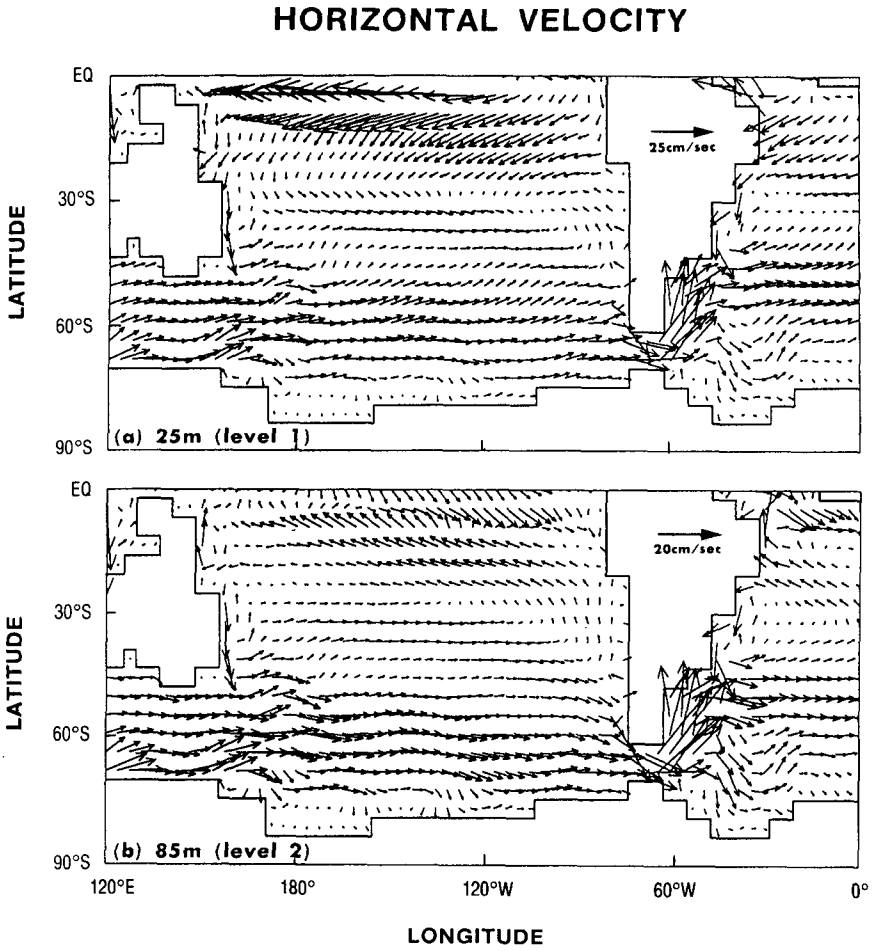

FIG. 4. Horizontal velocity at (a) 25-m and (b) 85-m depth in the ocean model. Notice that the velocity scales differ in each panel, as indicated by the standard vectors shown.

loss and deepening mixed layer seen in Figs. 3b and 3c.

The warm water entering from the East Australian Current ensures that the stratification of this column is initially very small in the top 300–400 m, and temperatures are warm, so that convective overturn can potentially extend to these depths as the water column moves along the path. Overturning is, however, controlled by the rather slow rate of heat loss to the atmosphere, so deepening occurs steadily along the path. Surface heat loss along the path is partly offset by the surface Ekman drift of cooler, fresher Antarctic water northward across the convective overturn band (Fig. 4a); this input has the effect of making both the temperature and salinity of the convective mixed layer (not shown) decrease along the flow path. The eastward cooling and freshening of these layers in the model is consistent with the eastward cooling and freshening of subantarctic mode water observed by McCartney (1977, see his Fig. 9).

Near the southern tip of South America, the convective layer deepens from 500 m to over 1000 m over only 1000 km distance along the flow path, or (since the column is moving eastward at about 0.05 m s^{-1}) within a time scale of order eight months. This is rather short compared to the expected equilibration time (Haney 1971) of $(\rho c_p H/\lambda)$, where ρ, c_p are the density and heat capacity of water, respectively, and H is the mixed-layer depth, which is about 20 months for the mixed layer 1000-m deep near South America. The rapid deepening near Cape Horn must therefore be due to the top 500 m being undercut by less dense water just below. Current maps like Fig. 4 in the depth range 500–1000 m (not shown) reveal southward movement along the South American coast near 60°S: this water is indeed less dense than water at the same depths near South America, on the axis of maximum convective depth in Fig. 3c. The inflow of relatively warm, light water at these levels permits rapid convective mixing to 1131-m depth (Fig. 3c) and enhanced surface heat loss in this region (Fig. 3b). There are strong analogies with the mechanism for formation of the Leeuwin Current off Western Australia, which also involves the formation of deep mixed layers (Godfrey

and Weaver 1991; Hirst and Godfrey 1993) near Australia's southwest corner, southward flow along the coast at one level, deep convective overturn, and northward and westward flows at a deeper level.

This discussion explains the formation of the Pacific branch of AAIW; however, the salinity minimum at 1131 m off Argentina (Fig. 2b) does not underlie a region of deep mixed layer (Fig. 3c) or a region of surface heat loss (Fig. 3b). Thus the AAIW advected away from this region must be formed elsewhere. Close comparison of Fig. 3c with Fig. 2c shows that at 1131-m depth, the region of deepest mixed layer SW of Cape Horn coincides with a bifurcation point in the currents: much of the water mass created in this region is swept around Cape Horn to travel northward in the Malvinas Current. Horizontal sections of vertical velocity in the surface levels of the model (not shown) indicate that downwelling also occurs along this path; it is vigorous enough in the region to carry water from the surface near Cape Horn to 1131-m depth near 45°S. However, the time scale for direct downwelling to renew AAIW is typically 30 years, based on a scale vertical velocity of 10^{-6} m s^{-1} in this region. Thus, the most likely source for the second salinity minimum in Fig. 2b is close to that for the first salinity minimum; that is, west and southwest of Cape Horn.

It may be noted that McCartney (1977, 1982) finds AAIW formation in the Scotia Sea, a few hundred kilometers east of Cape Horn. This does not occur in our model (Fig. 3c); however, comparison of the salinity plots of Fig. 2 suggests that the model currents bend northward after passing Cape Horn more rapidly in the model than in reality. These currents bring higher salinity water into the Scotia Sea, inhibiting convective overturn by stabilizing the water column near the surface. This would explain the absence of deep mixed layers in the Scotia Sea in the model.

Finally, it is worth noting the role that parameterized alongisopycnal mixing plays in maintaining a tongue of fresh AAIW in the model. Because the density surfaces in the Southern Ocean are steeply sloped, the model ocean diffuses low salinity surface water at the polar front into the ocean interior (England 1993), in spite of the broad region of Ekman divergence (Fig. 1) and associated upwelling near 60°S. Of course, this mechanism of AAIW formation is quite sensitive to the choice of the alongisopycnal diffusion coefficient (A_{HI}). In the present study A_{HI} is taken to be around 3×10^7 cm^2 s^{-1} in the surface 1000 m, based on observed estimates of typical eddy diffusion rates in the upper ocean (e.g., McWilliams et al. 1983; Thiele et al. 1986). With a typical meridional slope of isopycnal surfaces of 1000 m per 10° latitude in the Southern Ocean (or roughly 10^{-3}), a slope-squared dependence of A_{HV} on A_{HI} (Redi 1982) yields effective vertical diffusion rates of the order of $A_{HV} = 30$ cm^2 s^{-1} in the Southern Ocean. In the presence of an ambient upwelling rate of $w = 10^{-6}$ m s^{-1} in the circumpolar region (driven by the divergence of the surface Ekman drift; Fig. 1), we might expect the isopycnal diffusion term to act over depth scales of (A_{HV}/w) or 3000 m. In contrast, without an isopycnal mixing scheme in the ocean model, typical vertical diffusion rates in the surface 1000 m (0.3 cm^2 s^{-1}) limit the extent of isopycnal mixing in the circumpolar region (that is, in the presence of the wind-driven divergence) to only about 30 m. These scale arguments are evidenced in some of the experiments reported by England (1993), in which the isopycnal mixing scheme was required to ensure that an AAIW minimum was simulated at *each* longitude. Without an isopycnal mixing scheme, some latitude–depth sections in the Southern Ocean show only a subsurface salinity minimum (originating near the surface off southern Chile) *disconnected* from the surface salinity minimum at the polar front. Inclusion of isopycnal mixing acts to assimilate these water masses in spite of the ambient upwelling near 60°S. This renewal mechanism is similar to the isopycnal mixing scheme postulated by Molinelli (1981) from direct ocean measurements.

4. Conclusions

In summary, we find that the renewal of Antarctic Intermediate Water in an ocean general circulation model occurs without any direct subduction of surface water at the polar front. Instead, the large-scale advection and convective overturn of Subantarctic Waters is seen to renew the intermediate water north of the polar frontal zone, and in particular, in an isolated region off southern Chile. In addition, the model's approximate treatment of isopycnal mixing acts to diffuse low salinity water at the polar front into the interior of the ocean, in spite of a broad region of wind-driven upwelling in the Southern Ocean. This is quite unlike the traditional notion of direct circumpolar subduction of fresh surface water at the polar front.

REFERENCES

Broecker, W. S., 1991: The great ocean conveyor. *Oceanogr.*, **4**, 79–89.

Bryan, K., 1969: A numerical method for the study of the circulation of the world ocean. *J. Comput. Phys.*, **3**, 347–376.

Cox, M. D., 1984: *A primitive equation, three-dimensional model of the ocean.* Geophysical Fluid Dynamics Laboratory Ocean Group Tech. Rep. No. 1, 143 pp.

Deacon, G. E. R., 1937: The hydrology of the Southern Ocean. *Discovery Reps.*, Cambridge University Press, **15**, 1–124.

England, M. H., 1992: On the formation of Antarctic intermediate and bottom water in ocean general circulation models. *J. Phys. Oceanogr.*, **22**, 918–926.

——, 1993: Representing the global-scale water masses in ocean general circulation models. *J. Phys. Oceanogr.*, **22**, 1523–1552.

——, M. Tomczak, and J. S. Godfrey, 1992: Water-mass formation and Sverdrup dynamics; a comparison between climatology and a coupled ocean-atmosphere model. *J. Mar. Systems*, **3**, 279–306.

Esbenson, S. K., and Y. Kushnir, 1981: The heat budget of the global ocean: An atlas based on estimates from surface marine obser-

vations. Climate Research Institute, Oregon State University, Rep. No. 29, 27 pp.

Foster, T. D., and E. C. Carmack, 1976: Frontal zone mixing and Antarctic bottom water formation in the southern Weddell Sea. *Deep-Sea Res.*, **23,** 301–317.

Godfrey, J. S., and A. J. Weaver, 1991: Is the Leeuwin Current driven by Pacific heating and winds? *Progress in Oceanography,* Vol. 27, Pergamon, 225–272.

Gordon, A. L., 1986: Inter-ocean exchange of thermocline water. *J. Geophys. Res.*, **91,** 5037–5046.

Haney, R. L., 1971: Surface thermal boundary condition for ocean circulation models. *J. Phys. Oceanogr.*, **1,** 241–248.

Hellerman, S., and M. Rosenstein, 1983: Normal monthly wind stress over the world ocean with error estimates. *J. Phys. Oceanogr.*, **13,** 1093–1104.

Hirst, A. C., and J. S. Godfrey, 1993: The role of Indonesian throughflow in a global ocean GCM. *J. Phys. Oceanogr.*, **23,** 1057–1086.

Jacobs, S. S., R. G. Fairbanks, and Y. Horibe, 1985: Origin and evolution of water masses near the Antarctic continental margin: Evidence from $H_2{}^{18}O/H_2{}^{16}O$ ratios in seawater. *Oceanology of the Antarctic Continental Shelf,* S. S. Jacobs, Ed., Antarctic Research Series, Vol. 43, Amer. Geophys. Union, 58–86.

Levitus, S., 1982: *Climatological Atlas of the world ocean.* NOAA Prof. Paper 13, U.S. Dept. of Commerce, Washington, DC, 173 pp.

McCartney, M. S., 1977: Subantarctic Mode Water. *A Voyage of Discovery,* M. V. Angel, Ed., *Deep-Sea Res.*, **24**(Suppl.), 103–119.

——, 1982: The subtropical recirculation of Mode Waters. *J. Mar. Res.*, **40,** 427–464.

McWilliams, J. C., and Coauthors, 1983: The local dynamics of eddies in the western North Atlantic. *Eddies in Marine Science,* A. R. Robinson, Ed., Springer-Verlag, 92–113 pp.

Molinelli, E. J., 1978: Isohaline thermoclines in the southeast Pacific Ocean. *J. Phys. Oceanogr.*, **8,** 1139–1145.

——, 1981: The Antarctic influence on Antarctic Intermediate Water. *J. Mar. Res.*, **39,** 267–293.

Oberhuber, J. M., 1988: An atlas based on the "COADS" data set: The budgets of heat, buoyancy and turbulent kinetic energy at the surface of the global ocean. Max-Planck-Institut für Meteorologie, Report No. 15, 20 pp.

Pacanowski, R. C., K. W. Dixon, and A. Rosati, 1991: *The GFDL Modular Ocean Model users guide version 1.0.* Geophysical Fluid Dynamics Laboratory Ocean Group Tech. Rep. No. 2, 46 pp.

Redi, M. H., 1982: Oceanic isopycnal mixing by coordinate rotation. *J. Phys. Oceanogr.*, **12,** 1154–1158.

Sverdrup, H. U., M. W. Johnson, and R. H. Fleming, 1942: *The Oceans: Their Physics, Chemistry and General Biology.* Prentice-Hall, 1087 pp.

Thiele, G., W. Roether, P. Schlosser, R. Kuntz, G. Siedler, and L. Stramma, 1986: Baroclinic flow and transient-tracer fields in the Canary–Cape Verde Basin. *J. Phys. Oceanogr.*, **16,** 814–826.

Toggweiler, J. R., K. Dixon, and K. Bryan, 1989: Simulations of radiocarbon in a coarse-resolution world ocean model. I: Steady state prebomb distributions. *J. Geophys. Res.*, **94,** 8217–8242.